to note that a^N for the nitroxide, **13**, though somewhat solvent dependent,[41a] is also smaller than the a^N values found for acyclic acyl nitroxides (e.g.,[41a] it is 82-87% of the value found for $Me_3CN(O)COMe$). While ring-strain effects may contribute to the lowering of a^N in the cyclic amidyl and nitroxide, a more important factor would seem to be the improved delocalization of the unpaired electron from N to the carbonyl O in these radicals.

It is interesting to note that cyclic sulfonamidyls have N hfs and g values of 13.1-13.3 G and 2.0040-2.0042, respectively.[16-19] Their EPR parameters are therefore no different from those of acyclic sulfonamidyls (viz., a^N = 12.9-13.2 G and g = 2.0041-2.0044).[16,17,19]

Attempts to observe other cyclic amidyls (2-oxopyrrolidin-1-yl, 5-methyl-2-oxopyrrolidin-1-yl, and 2-oxopiperidin-1-yl) were frustrated by the poor solubility of the parent chloramides in cyclopropane at low temperatures.

Summary

N-Alkylcarboxamidyl radicals have a π-electronic ground state. Acyclic amidyls are either planar or nearly so when the N group is a primary or secondary alkyl but there is considerable rocking about the preferred conformation. Amidyls having an *N-tert*-butyl group are nonplanar, i.e., twisted, because of steric repulsion between the *tert*-butyl and the carbonyl oxygen atom.

Acknowledgment. We are grateful to Professor A. Berndt (Marburg) for his generous gift of 5,5-dimethylpyrrolidin-2-one. We are also pleased to acknowledge some very helpful comments by Drs. B. P. Roberts (London) and S. Glover (Port Elizabeth).

Supplementary Material Available: EPR parameters for amidyls at temperatures other than those listed in Table I (4 pages). Ordering information is given on any current masthead page.

Dehydration and Enolization Rates of Oxalacetate: Catalysis by Tertiary Amines

Mark Emly and Daniel L. Leussing*

Contribution from the Department of Chemistry, The Ohio State University, Columbus, Ohio 43210. *Received April 30, 1980*

Abstract: The hydration/dehydration and tautomerization rates of oxalacetate are subject to acid and base catalysis. H_2O and OH^- are much more effective for the former process than for the latter, but the opposite holds for tertiary amine catalysis. In buffers comprised of oxyanion bases or unsaturated amines, dehydration is significantly faster than tautomerization and remains so as the buffer concentration is varied. In dilute tertiary amine buffers dehydration rates are also faster, but as the buffer concentration increases, tautomerization rates increase rapidly and eventually surpass those for hydration/dehydration. It is this rate crossover which led earlier workers (ref 9) to propose a carbinolamine mechanism for tertiary amine-catalyzed tautomerization. After the rate crossover is taken into account, enolization is found to show linear rate-buffer concentration behavior with tertiary amines, vitiating the prime evidence cited for the carbinolamine mechanism. However, tertiary amine catalysis likely operates differently in the tautomerization and dehydration reactions.

Oxalacetate (oxac) is an important reactive substance which, because it is an intermediate in a number of crucial biological sequences, has been studied extensively. Fundamental to our understanding of oxac chemistry are the enolization and hydration reactions, shown in Scheme I, which may influence or may be mistaken for other reactions of interest.

While enolization has been investigated for many years,[1-9] relatively little attention has been focused on the solvational reactions. Kokesh[7] has determined the distribution of the components shown in Scheme I as a function of pH (38 °C) by using NMR band area measurements. Pogson and Wolfe[8] studied the rates of the enzymatic reduction of $oxac^{2-}$ at pH 7.4 (20 °C) with the goal of determining the concentrations of the components and their reaction rates. The hydrate content which they found is consistent with that reported by Kokesh,[7] and they established

Scheme I

$$^{-}O_2CC(OH)_2CH_2CO_2^{-} \overset{\text{slow}}{\rightleftharpoons} {}^{-}O_2CC(=O)CH_2CO_2^{-} \overset{\text{slow}}{\rightleftharpoons}$$

$$^{-}O_2CC(OH)=CHCO_2^{-} \overset{\text{fast}}{\rightleftharpoons} {}^{-}O_2CC(O^{-})=CHCO_2^{-}$$

enol enolate

that dehydration rates in tris or phosphate buffers are about 1 order of magnitude faster than enolization rates.

A reinvestigation of buffer catalysis on the enolization rates was recently reported by Bruice and Bruice.[9] These authors employed a pH jump technique to determine reaction velocities, and to circumvent interference from the presence of hydrate, which is dominant at low pH, adjusted the initial pH of the oxac solutions to 3.7. While they found normal linear rate vs. buffer concentration plots for catalysis by imidazole, pyridine, and oxyanion buffers, tertiary amines yielded plots showing two linear regions with the limb at higher buffer concentrations having the smaller slope. A multistep mechanism involving the formation of an intermediate carbinolamine was invoked to account for the indicated change in the rate-limiting step.

At the time that the paper by Bruice and Bruice[9] appeared an investigation of the effects of buffers and metal ions on oxac tautomerization rates was under way in our laboratories. Preliminary rate data obtained with *N,N,N',N'*-tetramethylethylenediamine (tetrameen) buffers containing Mg^{2+} gave no evidence of the two limbed plots. Because complexing metal ions

(1) A. Kornberg, S. Ochoa, and A. Mehler, *J. Biol. Chem.*, 159 (1948).
(2) B. E. Banks, *J. Chem. Soc.*, 5043 (1961); 63 (1962).
(3) G. W. Kosicki and S. N. Lipovac, *Can. J. Chem.*, **42**, 403 (1964).
(4) S. S. Tate, A. K. Grzybowski, and S. P. Datta, *J. Chem. Soc.*, **1372** (1964).
(5) E. Bamann and V. S. Sethi, *Arch. Pharm. (Weinhein, Ger.)*, **301**, 78 (1968).
(6) J. L. Hess and R. E. Reed, *Arch. Biochem. Biophys.*, **153**, 225 (1972).
(7) F. C. Kokesh, *J. Org. Chem.*, **41**, 3593 (1976).
(8) C. I. Pogson and R. G. Wolfe, *Biochem. Biophys. Res. Commun.*, **46**, 1048 (1972).
(9) Paula Y. Bruice and Thomas C. Bruice, *J. Am. Chem. Soc.*, **100**, 4793 (1978).

0002-7863/81/1503-628$01.00/0

have been observed to catalyze pyruvate hydration,[10] the possibility was suggested that the difference between our results and those reported in ref 9 was rooted in the solvational processes. We then focused further attention on the behavior toward oxac of tetrameen and two of the amines studied earlier,[9] 3-quinuclidinol and triethylamine, in the absence of complexing metal ions.

Enolization and dehydration rates were examined in detail for all three tertiary amines, and the rate laws for buffer catalysis were established. It was found that a rather complicated interplay exists between the two rate processes owing to marked differences in their sensitivities to tertiary amine catalysts. At low concentrations of tertiary amine, dehydration is faster than enolization, but the opposite order is obtained at high tertiary amine concentrations.

Experimental Section

Materials. Oxaloacetic acid (Sigma) was purified by recrystallization according to Bamann and Sethi[5] and stored under refrigeration. High-pressure LC chromatograms showed the white solid to be significantly purer than the original yellow solid. Titration with standardized NaOH confirmed the purity of the white solid to exceed 95%. 3-Quinuclidinol (Aldrich) was recrystallized from acetone. The hydrochloride salts of triethylamine (Baker) and *N,N,N',N'*-tetramethylethylenediamine (Aldrich) were prepared from the liquid amines and were recrystallized from water–acetone mixtures. Cl^- determinations indicated purities in excess of 98% for both amine hydrochloride salts. All solids were vacuum dried and stored over desiccant. Demineralized, doubly distilled water was used throughout; KOH, HCl, and KCl solutions were prepared in the usual manner. Potentiometric titrations were employed to determine the protonation constants of the amines. pH readings were determined by using a Radiometer Model 26 pH meter.

Kinetic Measurements. All kinetic determinations were performed at 25.0 ± 0.2 °C, μ = 0.25 (KCl). The Durrum-Gibson stopped-flow spectrophotometer, interfaced to a Nova minicomputer for data digitization and storage, was used throughout for kinetic measurements. The reactions were initiated by mixing two reactant solutions, one of oxaloacetate and the other of buffer, and the absorbancies at 260–280 nm were monitored. In one set of experiments (hereafter termed pH increase runs), oxac solutions initially at pH 1.0 were mixed with buffers containing excess alkali in sufficient amount to partially neutralize the acid and yield a buffer at some desired reaction pH. In another set of experiments (pH decrease runs) oxac solutions at pH 12.7 were mixed with buffers containing sufficient acid so that once again the final reaction mixture acquired the desired pH. The actual pHs of the reaction mixtures were experimentally determined separately by mixing 5-mL aliquots of the initial solutions and recording the pH of the mixture as soon as the electrode system stabilized (15–30 s).

The rate data were analyzed by determining the relaxation rate constant as each reaction process approached equilibrium. Consequently, it was not necessary to know the absolute values of absorbance as a function of time. For runs that possess biphasic rate character, the relaxation rate constants, $k_{i,obsd}$, were obtained from the data by a least-squares fit of the absorbance trace to an exponential decay equation of the form

$$A_t = A_\infty + A_1 e^{-k_{1,obsd}t} + A_2 e^{-k_{2,obsd}t} \quad (1)$$

where A_t is the measured relative absorbance at time t, A_∞ is the value at the completion of the reaction, and A_1 and A_2 are the amplitudes of each relaxation phase. One set of a replicate pair of experiments was used to collect absorbance–time points over the complete sequence of reactions; the second set of replicate experiments was used to collect points over the initial phase of the reaction. If the faster of the observed rate processes, designated here by $k_{1,obsd}$, was well separated from the slower of the observed rate processes, designated by $k_{2,obsd}$, then the slower time scan was analyzed as a single relaxation.

$$A_t = A_\infty + A_2 e^{-k_{2,obsd}t} \quad (2)$$

With use of the values of A_2 and $k_{2,obsd}$ so obtained, the faster time scan was then analyzed for A_1 and $k_{1,obsd}$ by using the full expression shown in eq 1. This procedure was not possible for cases in which the two relaxation processes were not well separated, and the full expression given in eq 1 was required to simultaneously obtain both rate constants. Monophasic absorbance changes were analyzed by using eq 2. For all experiments, values of the rate constants were taken as the average of six to eight replicate determinations.

(10) Y. Pocker and J. E. Meany, *J. Phys. Chem.*, **74**, 1486 (1970).

Computations. The reaction system described in Scheme I predicts that biphasic rate processes will occur under the influence of a perturbation. The perturbation employed here was a rapid change in pH effected by mixing oxac solutions with buffers at a different pH in the stopped-flow apparatus. Following the perturbation the system relaxes to the new equilibrium position, and from the absorbance–time traces, the (pseudo-) first-order relaxation rate constants, $k_{1,obsd}$ and $k_{2,obsd}$, were obtained as detailed above.

For the general case involving the two serial reversible reactions

$$1 \underset{k_{21}}{\overset{k_{12}}{\rightleftharpoons}} 2 \underset{k_{32}}{\overset{k_{23}}{\rightleftharpoons}} 3$$

the relationship between the individual stepwise rate constants and the theoretical relaxation rate constants $k_{i,calcd}$ is given by the expression in matrix notation

$$\begin{vmatrix} k_{12} - k_{i,calcd} & -k_{21} \\ -k_{21} + k_{32} & k_{21} + k_{23} + k_{32} - k_{i,calcd} \end{vmatrix} = 0$$

Cross multiplication followed by application of the quadratic equation gives eq 3, where $\Sigma = k_{12} + k_{21} + k_{23} + k_{32}$, $\Delta = k_{12} + k_{21} - (k_{23} + k_{32})$,

$$k_{i,calcd} = \tfrac{1}{2}(\Sigma \pm \sqrt{\Delta^2 + 4P}) \quad i = 1,2 \quad (3)$$

and $P = k_{21}k_{23}$. k_{21} and k_{32} are given by $k_{21} = k_{12}/K_{12}$ and $k_{32} = k_{23}/K_{23}$, where K_{12} and K_{23} are the equilibrium constants for the first and second processes, respectively. In the present investigation these constants have been determined independently.

The pH and buffer concentration dependence of k_{12} and k_{23} are described in terms of the second-order catalytic rate constants in the general equation.

$$k_{ij} = k_{ij,H}[H^+] + k_{ij,OH}[OH^-] + k_{ij,H_2O}[H_2O] + k_{ij,B}[B] + k_{ij,HB}[HB] \quad (4)$$

When the two relaxation rates differ by a sufficiently large factor (usually 1 order of magnitude or more), the coupling term $4P$ of eq 3 becomes negligibly small and the two limiting values of $k_{i,calcd}$ are

$$k_{i,calcd(+)} = k_{12} + k_{21} = k_{12}(1 + 1/K_{12}) \quad (5)$$

$$k_{i,calcd(-)} = k_{23} + k_{32} = k_{23}(1 + 1/K_{23}) \quad (6)$$

In this limit one of the $k_{i,calcd}$ determines the relaxation rate of the dehydration/hydration process and the other determines the relaxation rate of the enolization/ketonization process. The second-order catalytic rate constants may be obtained from a set of data through a linear least-squares fitting procedure in which the sum of the squares of the differences $k_{i,obsd} - k_{i,calcd}$ is minimized. Graphical procedures are also convenient. It is important to realize that before a rate assignment can be made an ambiguity in the observed rates must first be resolved. It is not valid merely on the basis of their order to assign the first relaxation to dehydration/hydration and the second to enolization/ketonization. Additional information is necessary to make the assignment. The signs and magnitudes of absorbance changes are often useful for this purpose but need not be the sole means of removing the ambiguity. Other types of data, e.g., other types of rate determinations, may also be employed.

When the rates of the two relaxations lie close together, then the term $4P$ is not negligible. In this circumstance each relaxation is comprised of components of both processes. Nonlinear curve fitting techniques must then be employed to obtain the second-order catalytic rate constants from the data set. One such technique employed successfully for a number of years in our laboratory has been described by Bevington.[11]

Equations 3, 5, and 6 imply an important property of this general reaction system: the relaxation rate constants will be the same regardless of which direction the new equilibrium position is approached.

Results and Discussion

With use of NMR band area[7] and UV absorbance measurements,[12] the distributions of oxac among hydrate, keto, and enol forms in solutions at various pH at 25 °C were determined,[13] and the results are given in Table I. In agreement with the earlier workers,[7,8] extensive hydration was found in acidic solutions where H_2oxac is the predominant species. As oxac is deprotonated, the degree of hydration at equilibrium progressively decreases. The equilibrium enol/keto ratio also decreases at first but then increases

(11) Phillip R. Bevington, "Data Reduction and Error Analysis for the Physical Sciences", McGraw-Hill, New York, 1969.
(12) J. L. Hess and R. E. Reed, *Arch. Biochem. Biophys.*, **153**, 226 (1972).
(13) H. S. Mao and B. Lillis, results obtained in these laboratories.

Table I. Equilibrium Distribution of Oxalacetate as a Function of pH[a] at 25 °C

pH	% keto	% hydrate	% enol	hyd/keto	enol/keto
0.0	sm	95	5		
1.0	8	85	7	10.6	0.875
3.1	55	35	10	0.64	0.18
3.7	65	25	10	0.38	0.15
4.7	76	13	11	0.17	0.14
6.9	81	7	12	0.09	0.15
12.7	73	6	21[b]	0.08	0.29

[a] $pK_{1a} = 1.93$, $pK_{2a} = 4.0$, $pK_{3a} = 13.7$.[4] [b] enol + enolate.

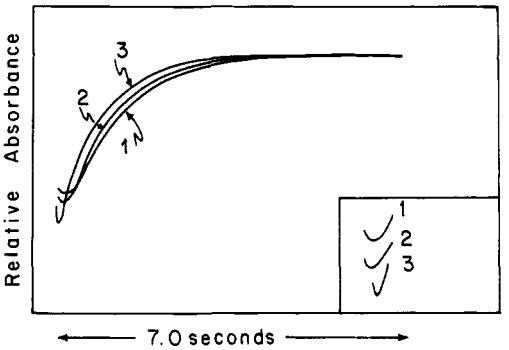

Figure 1. Absorbance–time traces for pH jump experiments into 3-quinuclidinol buffers (initial pH of oxac solution = 1.0; final pH of mixed solution = 10.0; 1.5 mM oxac): 1, 10 mM quinuclidinol; 2, 20 mM quinuclidinol; 3, 120 mM quinuclidinol (265 nm). The inset shows the initial phases of the reactions drawn by using an expanded scale. The curves have also been displaced for clarity.

sharply in highly alkaline solutions where the enolate ion is formed.[3,4]

In the pH increase runs the oxac solutions were initially at pH ~1 where hydrate is the dominant component. When the pH is rapidly increased to 4.5 and above, the H_2(oxac) protons are rapidly neutralized and the $oxac^{2-}$ system relaxes to a new equilibrium distribution of hydrate, keto, and enol. Figure 1 shows absorbance–time traces obtained from pH increase runs into 3-quinuclidinol buffers at differing concentrations, but all giving a final reaction pH of about 10.1. In each trace the expected biphasic process is manifested as an initial absorbance decrease followed by a substantial absorbance increase (the ordinate of Figure 1 covers a range of about 2 absorbance units). The initial absorbance decrease arises from the true chemical behavior of each reaction system and is not an instrumental artifact: the dead time of the stopped-flow appratus is less than 10 ms; triggering occurred at the instant flow ceased and not before; pH jump experiments run on blanks containing buffers and indicators showed "instantaneous" reaction rates on the same time scale; the behavior observed in Figure 1 has not been seen with our instrument in other reaction systems known to be monophasic.

In the pH decrease runs the enolate oxygen atom is rapidly protonated,[9] and the system relaxes to a new equilibrium position which contains less enol. The data of Table I show that as long as the final solution pH is at 5 or above, changes in the hydrate content of the oxac amount to less than 1% and are negligible for all practical purposes. Although the reaction remains biphasic in principal, the amplitude of the hydrate ⇌ keto reaction is so small that this process is not observed. Without ambiguity, the only absorbance change that is observed is that for the reaction keto ⇌ enol. In Figure 2 are shown absorbance–time traces in which oxac solutions at pH 12.7 were mixed with 3-quinuclidinol buffers to give a series of solutions having the same final compositions as those described in the legend of Figure 1. In accordance with expectations only monophasic traces were obtained, and this was verified by the close agreement of the curves to eq 2.

The rate curves displayed in Figures 1 and 2 show that in these 3-quinuclidinol buffers the rate of establishment of the keto ⇌ enol equilibrium is faster than that of the hydrate ⇌ keto equilibrium. Qualitatively, the absorbance changes shown in Figure 2 occur over the same time range as the initial absorbance decreases observed in Figure 1, and the quantitative agreement is very good. The two relaxation rate constants obtained from each of the pH increase runs into the 3-quinuclidinol buffers are given in Table II along with those for the corresponding keto ⇌ enol relaxations shown in Figure 2. It is seen for a given buffer the last relaxation rate constant agrees with the larger of the two determined from the pH increase run.

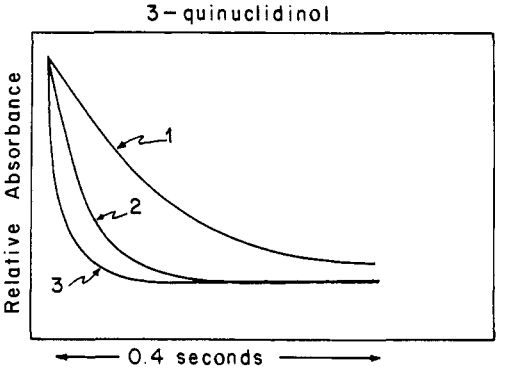

Figure 2. Absorbance–time traces for pH jump experiments into 3-quinuclidinol buffers (initial pH of oxac solution = 12.7; final pH of oxac solution = 10.1; 1.5 mM oxac): 1, 10 mM quinuclidinol; 2, 60 mM quinuclidinol; 3, 120 mM quinuclidinol (265 nm).

Table II. Observed Relaxation Rate Constants from Some pH Jump Experiments at 25 °C

reaction conditions		pH jump mode		
		increase[a]		decrease[b]
buffer	pH	$k_{1,obsd}$, s^{-1}	$k_{2,obsd}$, s^{-1}	k_{obsd}, s^{-1}
0.020 M tetrameen	7.22	1.89	0.37	
0.030 M tetrameen	7.00			2.33
0.060 M tetrameen	7.25	5.19	0.41	4.54
0.100 M tetrameen	7.24			7.82
0.105 M tetrameen	7.35	8.47	0.46	
0.020 M tetrameen	5.34	1.27	0.46	
0.025 M tetrameen	5.42			1.04
0.040 M tetrameen	5.37	2.23	0.61	
0.050 M tetrameen	5.43			1.99
0.060 M tetrameen	5.38	3.41	0.64	
0.010 M 3-quinuclidinol	10.12	3.7	1.19	3.06
0.040 M 3-quinuclidinol	10.03	13.8	1.28	12.3
0.080 M 3-quinuclidinol	10.0	28.1	1.42	24.4
0.010 M triethylamine	11.04		1.66	1.62
0.050 M triethylamine	11.3	14.5	6.89	7.82
0.090 M triethylamine	11.35	22.3	10.4	15.4

[a] Initial pH of oxac solution was 1.0. [b] Initial pH of oxac solution was 12.7.

The signs and amplitudes of the absorbance changes shown in Figure 1 also lead to this same conclusion. Table I shows that at pH 1.0 85% of the oxac is hydrated and the enol/keto ratio is 0.88. At pH 10.1 the distribution is essentially the same as that recorded for pH 6.9: 7% hydrate and an enol/keto ratio of 0.15. Because it is only the concentration of enol that is followed at 265 nm, Figure 1 shows that after forming $oxac^{2-}$ by neutralizing H_2(oxac), the enol content first decreases in an attempt to establish the new enol/keto ratio before appreciable dehydration occurs. As slower dehydration generates more keto the faster keto ⇌ enol reaction follows along and a corresponding increase in enol results. The larger amplitude of the slower absorbance increase shows that although this change represents an increase in enol, the rate is associated with a change in the concentration of the dominant species initially present, i.e., the hydrate.

Still another line of evidence supports the present assignment of reaction rates. Enolization can be induced at a constant pH in neutral buffers (where changes in hydrate are negligible) by

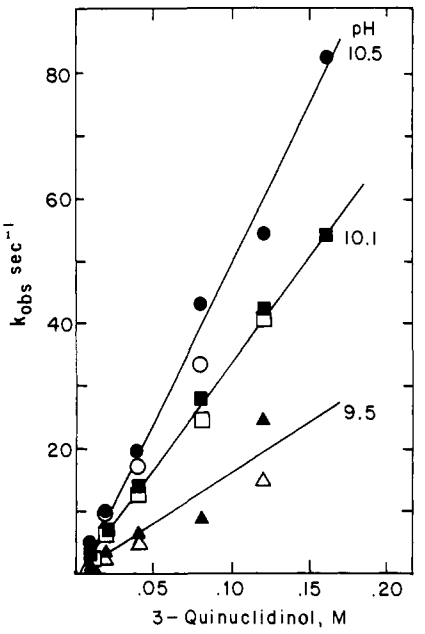

Figure 3. Enolization rate constant as a function of the 3-quinuclidinol concentration (open points, initial oxac pH 12.7; filled points, initial oxac pH 1.0 (fast component of the biphasic rates)): ○, pH 10.4; ●, pH 10.5; □, pH 10.1; ■, pH 10.1; △, pH 9.5; ▲, pH 9.4. Solid lines are theoretical.

mixing solutions of $oxac^{2-}$ with a complexing metal ion in the same buffer. The rate law for the conversion of $oxac^{2-}_{keto}$ to complexed $oxac^{2-}_{enol}$ exhibits both metal ion-dependent and metal ion-independent terms. The values of the rate constants associated with the metal ion-independent paths have been found to be identical with those assigned here to enolization.[14]

In addition to the results presented for the 3-quinuclidinol buffers, Table II gives the results for similar series of experiments performed in triethylamine and tetrameen buffers. In tetrameen the rates are seen to be ordered the same as in 3-quinuclidinol: keto $\rightleftharpoons$ enol > hydrate $\rightleftharpoons$ keto. The order in the triethylamine buffers at pH >11 is reversed, however. As is shown below where the results over a wider range of pH and buffer concentrations are discussed, the two rate processes differ greatly in their sensitivities to the nature of the catalysts: dehydration is catalyzed by H_2O and OH^- to a greater extent than is enolization, but the latter reaction is considerably more sensitive to the presence of aliphatic tertiary amines than the former. Thus, dehydration is normally faster than enolization, but the tertiary amine catalysts may easily cause this order to be reversed, unless the solutions are fairly alkaline.

Tautomerization rate constants obtained over a wide range of 3-quinuclidinol concentrations are shown plotted in Figure 3 for pH decrease runs (open circles) and pH increase runs (closed circles). At a given pH the rate constants for the two types of experiments are once again seen to be in good agreement with each other and exhibit the same linear buffer dependence. Bruice and Bruice[9] in similar plots report a pronounced change in slope in the vicinity of 0.05 M 3-quinuclidinol, but such behavior is not observed here. In fact, the lines defined by our data correspond roughly to linear segments drawn through the rates shown at low buffer concentrations in Figure 10 of ref 9. Furthermore, the slower rates shown at high buffer concentrations in this earlier work agree well with those we identify as arising from dehydration. It appears that a rate reversal has influenced the earlier observations.

In order to test this hypothesis, we performed pH jump experiments with the oxac solutions initially at pH 3.7 but used higher oxac concentrations in order to better resolve the initial stages of the reaction. In Figure 4 are shown absorbance–time traces obtained from experiments in which the initial oxac pH

(14) Mark Emly and Daniel L. Leussing, to be submitted for publication.

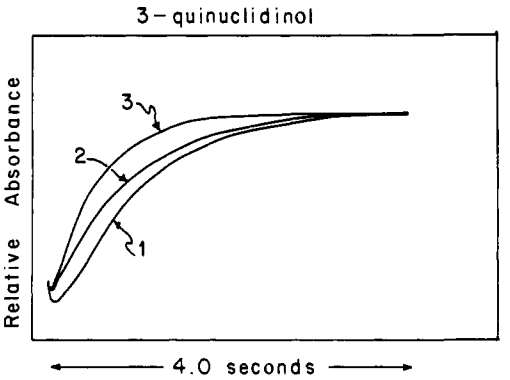

Figure 4. Absorbance–time traces for pH jump experiments into 3-quinuclidinol buffers (initial pH of oxac solution = 3.7). All other conditions are the same as described in the legend of Figure 1 except oxac is 4.5 mM.

was 3.7 and the final buffer concentrations and pH were identical with those used in Figure 1. It is quite clear that the curves shown in Figure 4 are biphasic and strongly resemble those shown in Figure 1. One important difference exists between the two sets of experiments, however: the concentrations of oxac employed in obtaining the curves of Figure 4 were 3 times those used for the Figure 1 runs. The higher oxac concentrations were necessary to match the amplitudes of the slow processes with those shown in Figure 1. Since oxac at pH 3.7 is calculated to have a hydrate content of 25% (Table I), these amplitudes are therefore found to be roughly proportional to the initial hydrate concentration (85% under the conditions described in Figure 1), as they must be if the interpretation proposed here is correct. In the earlier experiments Bruice and Bruice employed lower oxac concentrations and a higher reaction temperature (30 °C). This combination would cause it to be very difficult to ascertain the presence of two reactions. We have found, however, that the absorbance–time traces obtained by using dilute buffers under their conditions are better fit to the two-term exponential decay, eq 1, than to the equation for a single decay, eq 2.

The observation of a biphasic absorbance change does not in itself rule out a carbinolamine mechanism, because this would also yield biphasic behavior, provided the carbinolamine were formed in sufficiently high concentrations to influence the absorbance. However, the results shown in Figures 1 and 4 are not consistent with this interpretation, because they show that it is the *initial* conditions that influence the amplitudes. A rate involving carbinolamine would be a function only of the mixed solution, and changes in the oxac level would not be required to maintain constant amplitudes as the initial pH of this reactant solution is varied. The inclusion of carbinolamine into Scheme I would cause the system to exhibit triphasic behavior unless this intermediate were formed only at very low concentrations.

In Figure 5 are presented the faster of the relaxation rate constants obtained from pH increase runs into tetrameen buffers (filled points) and the rate constants for the monophasic rates obtained from pH decrease runs (open points). Once again very good agreement between these two sets of data and linearity with buffer concentrations is observed. Owing to the presence of two relaxations which must be resolved from the absorbance–time traces, the values from the pH increase runs tend to show more scatter. In computing the catalytic rate constants for enolization the pH decrease runs were weighted more heavily.

The relaxation rate constants for only pH decrease runs into triethylamine buffers are shown in Figure 6 while both sets of relaxation rate constants obtained from the pH increase runs are plotted in Figure 7. These last values lie so close to each other that they possess components from both processes in accordance with eq 3. In Figure 7 the points having the greater enolization component are shown as open and those mostly comprised of dehydration are shown as filled.

The enolization rate data were resolved into acid–base-catalysis terms as described above. Amine (B)-catalyzed pathways were

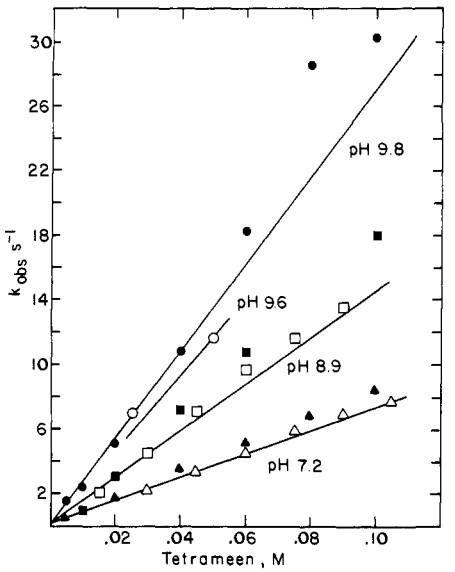

Figure 5. Enolization rate constant as a function of tetrameen concentration: open points, initial oxac pH 12.7; filled points, initial oxac pH 1.0 (faster component). Solid lines are theoretical.

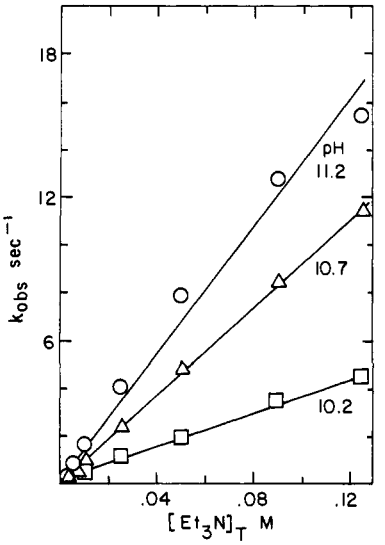

Figure 6. Enolization rate constant as a function of triethylamine concentration (initial oxac pH 12.7). Solid lines are theoretical.

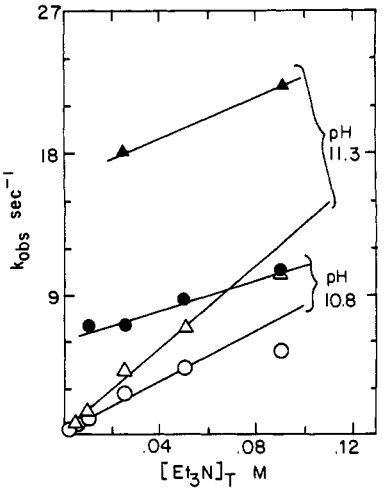

Figure 7. Enolization and dehydration rate constants as a function of the triethylamine concentration (initial oxac pH 1.0 (both components of biphasic reaction)): ●, dehydration, pH 10.8; ○, tautomerization, pH 10.8; ▲, dehydration, pH 11.3; △, tautomerization, pH 11.3.

Table III. Catalytic Rate Constants for the Tautomerization of Oxalacetate Dianion at 25 °C

$$B + oxac^{2-}_{keto} \underset{k_{-2}}{\overset{k_2}{\rightleftharpoons}} oxac^{2-}_{enol} + B$$

catalyst (B)	pK_a^{HB}	rate constants, M^{-1} s^{-1} k_2	k_{-2}	$k_2 + k_{-2}$
OH^-	15.7	80	520	600
Et_3N	10.9	22	148	170
3-quinuclidinol	10.1	87	573	660
tetrameen	9.35	41	282	313
H(tetrameen)$^+$	6.15	10	66	76
H_2(tetrameen)$^{2+}$		3.5	22.5	26

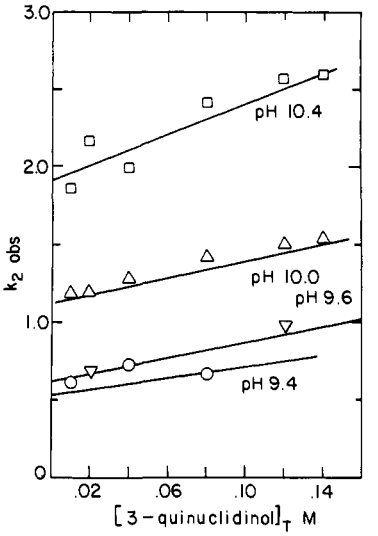

Figure 8. Dehydration rate constant as a function of 3-quinuclidinol concentration (initial oxac pH 1.0 (slower component of biphasic reaction)). Solid lines are theoretical.

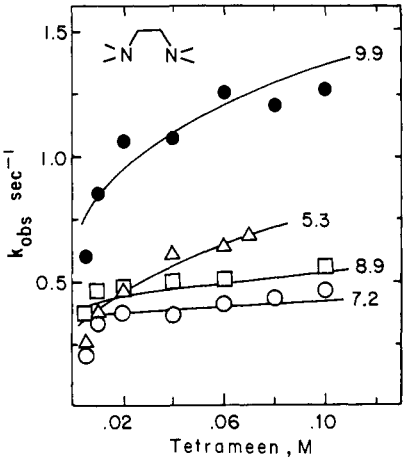

Figure 9. Dehydration rate constant as a function of the tetrameen concentration (initial oxac pH 1.0). Solid lines are theoretical.

found to be important with all three amines, and OH^- catalysis was especially pronounced with triethylamine. Only with tetrameen were contributions from the protonated species, H_2(tetrameen)$^{2+}$ and H(tetrameen)$^+$ found to be important. In agreement with Bruice and Bruice[9] we found no evidence for the presence of cross terms such as $k_{HB,B}$[HB][B]. The catalytic rate constants are given in Table III.

Dehydration relaxation rate constants plotted as a function of buffer concentration are shown in Figure 8 for 3-quinuclidinol and in Figure 9 for tetrameen. The curvature shown at low buffer concentrations in Figure 9 arises from systematic changes in the final pH of the reaction solutions as the buffer concentration was increased. These pH changes were taken into account in evalu-

Table IV. Catalytic Rate Constants for the Dehydration and Hydration of Oxalacetate Dianion at 25 °C

$$B + oxac_{hyd} \underset{k_{-1}}{\overset{k_1}{\rightleftharpoons}} B + oxac_{keto}$$

catalyst (B)	pK_a^{HB}	k_1, M^{-1} s^{-1}	k_{-1}, M^{-1} s^{-1}	$k_1 + k_{-1}$, M^{-1} s^{-1}
OH^-	15.7	6.5×10^3	500	7.0×10^3
Et_3N	10.9	69	6	75
3-quinuclidinol	10.1	6.6	0.6	7.2
tetrameen	9.35	2.3	0.2	2.5
H_2-(tetrameen)$^{2+}$		5.1	0.4	5.5
H_2O	−1.7	6.3×10^{-3}	0.5×10^{-3}	6.8×10^{-3}

ating the second-order rate constants for the catalytic pathways. The data analysis again revealed the presence of amine and OH^- catalysis. With tetrameen which covered the lowest pH range investigated catalysis by H_2(tetrameen)$^{2+}$ and H_2O was also found. The catalytic rate constants for dehydration are given in Table IV.

Pogson and Wolfe[8] determined oxac dehydration and enolization rates in buffers at pH 7.4. For 0.10 M phosphate the sum of their forward and backward dehydration rate constants (which corresponds to the relaxation rate constant determined here) is 0.48 s^{-1}. The excellent agreement with the value 0.41 s^{-1} which we found for dehydration in 0.06 M tetrameen at pH 7.25 ($k_{2,obsd}$ in Table II) further strengthens our conclusions.[15] They also found that the enolization rate in the phosphate buffer is about 1 order of magnitude slower than dehydration, consistent with Bruice and Bruice's conclusions regarding enolization rates in buffers comprised of oxygen donor atoms. In contrast, Table II shows that in the 0.060 M tetrameen buffer at pH 7.25 enolization is 1 order of magnitude faster than dehydration.

The rate behavior in the oxyanion buffers is straightforward, and the buffer dependence of the enolization rates may be determined without complications. In this regard excellent agreement between our work and that reported in ref 9 supports the present assignments. From the pH dependence of the enolization rates in oxyanion buffers, Bruice and Bruice obtained a value of 6×10^2 M^{-1} s^{-1} for OH^- catalysis. From the pH dependence of the rate that we have assigned to enolization in tertiary amine buffers, a corresponding value of 5×10^2 M^{-1} s^{-1} was extracted.

From the catalytic effects of H_3O^+, HOAc, $H_2PO_4^-$, pyridinium ions, and imidazolium ions on oxac enolization rates, Bruice and Bruice obtained a Brønsted α of −0.43. The second-order rate constant which we have found for H_2(tetrameen)$^{2+}$ catalysis lies close to the straight line in the Brønsted plot defined by these buffers (after a statistical correction of 2.0 is applied) showing that H_2(tetrameen)$^{2+}$ acts as a general-acid catalyst in this reaction. H(tetrameen)$^{2+}$, on the other hand, has a higher catalytic rate constant in spite of its much lower acidity, indicating that it essentially functions as a base catalyst.

A Brønsted plot for base-catalyzed enolization is shown in Figure 10. The rates for the oxyanion buffers and imidazole were taken from ref 9, but those for the tertiary amines have been determind here. Quite clearly and in complete agreement with Bruice and Bruice, the tertiary amines are seen to be much better catalysts for enolization than are the other buffers. Furthermore, the tertiary amines appear to have a smaller β, so that relative

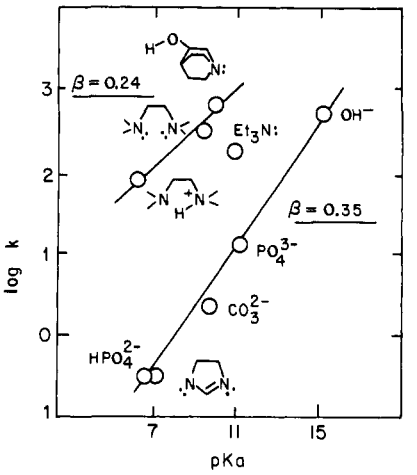

Figure 10. Brønsted plot of the enolization rate constants. The data points for the tertiary amine were determined in this work; the others were taken from ref 9.

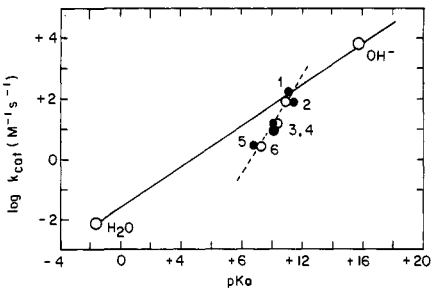

Figure 11. Brønsted plot of the dehydration rate constants (O, this work; ●, ref 9 (assigned to carbinolamine formation)): 1, quinuclidine; 2, triethylamine; 3, 3-quinuclidinol; 4, trimethylamine; 5, chloroquinuclidine; 6, tetrameen.

to its basicity, H(tetrameen)$^+$ is the best catalyst. Whether, or not, the high activities of the tertiary amines arise from a mechanism involving low concentrations of an intermediate carbinolamine is not directly answered by the present results. Although such a mechanism is possibly operational, it is important to bear in mind the well-known fact that solvational energies in polar solvents cause the proton basicities of tertiary amines to be significantly lower than their intrinsic gas-phase basicities. If little charge transfer occurs in the transition state then the gas-phase basicities would be a better measure of the catalytic effect.[17]

The dehydration rates also are subject to buffer catalysis. OH^- is much more effective for these reactions than it is for enolization, and even H_2O is observed to function as a base catalyst. Regarding catalysis by these two species our results are once again in excellent agreement with those of the earlier report.[9] By extrapolating to zero concentration the rates they assigned to carbinolamine formation, i.e., those obtained at high tertiary amine concentration, Bruice and Bruice found solvent dependent rates adhering to the expression

$$k_{obsd}(\text{zero buffer}) = 0.39 + 9.9 \times 10^3[OH^-] \quad (30\ °C)$$

From Table IV, the corresponding equation is

$$k_{obsd}(\text{zero buffer}) = 0.38 + 7.8 \times 10^3[OH^-] \quad (25\ °C)$$

This agreement provides additional strong support for the conclusion that the rates measured at higher concentrations of tertiary amine buffers in the earlier study are the same as those we assign to dehydration.

(15) Pogson and Wolfe (ref 8) found somewhat higher rates in tris buffers. Contrary to an earlier claim (ref 2) they report no evidence for Schiff base formation between $oxac^{2-}$ and the primary amine. Monoprotonated ethylenediamine is only slightly less basic than tris, and work in our laboratories (ref 16) has established that on the same time scale as required for dehydration and tautomerization $(en)H^+$ reacts with $oxac^{2-}$ to form both imine and enamine. It may be that the discrepancies in rates between phosphate and tris buffers reported by Pogson and Wolfe arise from interference by these species. The differences in enol and hydrate contents of oxac solutions reported here and by Pogson and Wolfe in phosphate are consistent with the temperature differences between these two studies.

(16) Daniel L. Leussing and N. V. Raghavan, *J. Am. Chem. Soc.*, **102**, 5635 (1980).

(17) Reviewer II proposes that an electrostatic interaction could account for at least part of the difference between tertiary amines and oxyanion bases. In the transition state the positively charged protonated tertiary amine will be stabilized by electrostatic interaction with the several negative charges of the substrate. There is no such electrostatic stabilization for the transition state for oxyanion catalysts.

A Brønsted plot of the dehydration rate constants is shown in Figure 11. The points for base catalysis by H_2O and OH^- define a line yielding a Brønsted β of 0.34. This is essentially the same value reported by Bruice and Bruice for the catalytic effect of oxyanion bases on enolization, but the dehydration rates are displaced to higher values by 1.1 log units. Therefore, in these "normal" buffers dehydration is likely to be always faster than enolization regardless of buffer concentration and no rate crossover will be observed.

Also, plotted in Figure 11 are the rate constants determined here for tertiary amine-catalyzed dehydration together with those taken from ref 9 which have been assigned to carbinolamine formation. It is seen that the two sets of constants are virtually identical, once again providing evidence that the rates of the same process have been measured in these two studies.

The rate constants found for triethylamine and quinuclidine catalysis are observed in Figure 11 to lie close to the line drawn through the points for H_2O and OH^-, which appear to define an upper limit on catalysis. The other tertiary amines show sharply decreasing catalytic effectiveness as their basicity decreases. The dashed line drawn through the tertiary amine data points has a slope of 1.4. Although tertiary amine bases are excellent catalysts for tautomerization, unless they are strongly basic they are seen to be poor catalysts for the solvational processes. Thus, in tertiary amine buffers at low concentration, dehydration rates are faster than those for tautomerization, but as the tertiary amine concentration increases, the enolization velocities become markedly faster and eventually surpass the dehydration rates. It is this behavior which accounts for the change in slope noted by Bruice and Bruice.[9]

The difference in sensitivity to tertiary amines likely reflects the operation of two essentially different mechanisms. In enolization, the tertiary amine is required to approach the substrate closely in order to promote the removal of a proton from the carbon atom

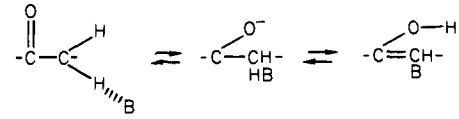

while in hydration an intervening H_2O molecule likely is required

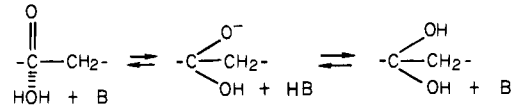

An OH^- ion could, of course, directly attack the carbon atom of the carbonyl group.

Acknowledgment. This research was supported by the National Science Foundation Grant No. CHE77-14637.

Exciplex Emissions of Intra- and Intermolecular Benzophenone and *N,N*-Dimethylaniline Systems

Hiroshi Masuhara,*‡ Yasuhiro Maeda,‡ Hirochika Nakajo,‡ Noboru Mataga,*‡ Kyoichi Tomita,† Hitoshi Tatemitsu,† Yoshiteru Sakata,*† and Soichi Misumi†

Contribution from the Department of Chemistry, Faculty of Engineering Science, Osaka University, Toyonaka, Osaka 560, Japan, and the Institute of Scientific and Industrial Research, Osaka University, Suita, Osaka 565, Japan. *Received December 7, 1979*

Abstract: Emission spectra of intra- and intermolecular exciplex systems of benzophenone and *N,N*-dimethylaniline were studied in detail at low temperature. Two new emissions were observed for the first time in the present work in addition to the well-known phosphorescence of the CT complex formed in the ground state. The first emission has a lifetime of a few tens nanoseconds, which is common to intra- and intermolecular systems. The second emission with a longer lifetime than that of the first one is obtained only in the case of the intramolecular system. A possibility that these emissions are due to fluorescent products was examined. Considering solvent, temperature, and concentration dependences of these emissions, it is proposed that the first and the second emissions are due to the singlet and the triplet exciplexes, respectively. Dynamic behaviors and geometrical structures of these exciplexes are discussed.

Introduction

Hydrogen abstraction by the triplet benzophenone from amines is well-known as a typical organic photochemical reaction which proceeds with a large rate and a high quantum yield. With examination of the kinetic data, it has been concluded that this reaction occurs through the triplet exciplex state.[1] Namely, charge transfer (CT) from amines to the triplet ketone is induced at first, which is followed by proton transfer. More direct information on this CT intermediate state has been given by the following two types of studies. The first is flash-photolysis studies giving absorption spectra of transient species. The benzophenone anion and the amine cation dissociated from the exciplex were first observed in strongly polar solvents.[2] Detailed laser-photolysis studies confirmed the competing processes of ionic dissociation and proton transfer in the CT state formed immediately after quenching reaction.[3] Rapid electron transfer was also demonstrated for the intramolecular benzophenone–*N,N*-dimethylaniline (DMA) system by a picosecond laser-photolysis method.[4] However, no distinct absorption spectra of the triplet exciplex have been reported at the present stage of investigation.

The other study on the CT intermediate is to observe emissions of the relevant CT complexes stable in the ground state. Arimitsu

‡Osaka University, Toyonaka.
†Osaka University, Suita.

(1) S. G. Cohen, A. Parola, and G. H. Parsons, *Chem. Rev.*, **73**, 1141 (1973). R. S. Davidson in "Molecular Association", Vol. 1, R. Foster, Ed., Academic Press, London, 1975.
(2) R. F. Bartholomew, R. S. Davidson, P. F. Lambeth, J. F. McKellar, and P. H. Turner, *J. Chem. Soc., Perkin Trans. 2*, **2**, 577 (1972).
(3) S. Arimitsu and H. Masuhara, *Chem. Phys. Lett.*, **22**, 543 (1973); S. Arimitsu, H. Masuhara, N. Mataga, and H. Tsubomura, *J. Phys. Chem.*, **79**, 1255 (1975).
(4) H. Masuhara, Y. Maeda, N. Mataga, K. Tomita, H. Tatemitsu, Y. Sakata, and S. Misumi, *Chem. Phys. Lett.*, **69**, 182 (1980).

0002-7863/81/1503-634$01.00/0